



Seasonal rainfall pattern using coupled neural network-wavelet technique of southern Uttarakhand, India

Shekhar Singh¹ · Deepak Kumar¹ · Dinesh Kumar Vishwakarma² · Rohitashw Kumar³ · Nand Lal Kushwaha^{4,5}

Received: 13 March 2022 / Accepted: 18 March 2024 / Published online: 28 March 2024
© The Author(s), under exclusive licence to Springer-Verlag GmbH Austria, part of Springer Nature 2024

Abstract

Hydrological data is crucial for accurate forecasting of precipitation which can be used for water resources planning and management. The purpose of this study is to develop a seasonal rainfall forecast model, using a hybrid wavelet-artificial neural network (WANN) model based on regression analysis to predict seasonal rainfall in Almora, Lansdown, Kashipur and Mukteswar region in Uttarakhand (India). The statistical results shows that the mean maximum rainfall was found to be 746.82 mm, 1586.58 mm, 1060.53 mm and 964.43 mm for Almora, Lansdown, Kashipur and Mukteswar, respectively. The models WANN-03 (Network 4–8-1), WANN-10 (Network 4–7-1), WANN-10 (Network 4–7-1) and WANN-15 (Network 4–8-1) were found to be the most efficient models for Mukteswar, Lansdown, Kashipur and Almora, based on the high coefficient of determination (R^2) and coefficient of efficiency (CE) values and low root mean square error (RMSE) values that were obtained using each model. For each season, four WANN models have been developed (total of sixteen models) by varying the number of hidden neurons. The results shows that only one WANN model was not sufficient to predict the rainfall of all stations. Every station has a specific networked model which could model the data more precisely. The findings illustrated that the hybrid model of WANN having Network (4–7-1) was found most superior model ($R^2 = 0.857$, $RMSE = 32.192$ and $CE = 0.846$) for the Lansdown stations among all the stations.

✉ Dinesh Kumar Vishwakarma
dinesh.vishwakarma4820@gmail.com

✉ Rohitashw Kumar
rohituhf@rediffmail.com

Shekhar Singh
shekharsingh861@gmail.com

Deepak Kumar
deepak.swce.cot.gbpuat@gmail.com

Nand Lal Kushwaha
nand.kushwaha@icar.gov.in

¹ Department of Soil and Water Conservation Engineering, Govind Ballabh Pant University of Agriculture & Technology, Pantnagar, Uttarakhand 263145, India

² Department of Irrigation and Drainage Engineering, Govind Ballabh Pant University of Agriculture and Technology, Pantnagar, Uttarakhand 263145, India

³ College of Agricultural Engineering and Technology, Sher-e-Kashmir University of Agricultural Sciences and Technology of Kashmir, Jammu and Kashmir 190025, Srinagar, India

⁴ Division of Agricultural Engineering, ICAR-Indian Agricultural Research Institute, New Delhi 110012, India

⁵ Department of Soil and Water Engineering, Punjab Agricultural University, Ludhiana, Punjab 141004, India

1 Introduction

Climate change is a matter of concern and changing patterns in rainfall are one of the most important parameters affecting climate (Thomas et al. 2007). It is a severe problem for today's scientific community and it deserves attention. In the Asian region, the climate change had directly influenced the streamflow volume and temporal distribution, which resulted in an increase of the stress level of water resources (White et al. 2014; Lu et al. 2024). The distribution of rainfall is indeed influenced by the relief, or topography, of a country (Oettli and Camberlin 2005; Kushwaha et al. 2021; Li et al. 2020). The north-eastern state of India receives rainfall more than 500 mm of annual rainfall (Kripalani et al. 1996; Wu et al. 2022) while in desert areas like Rajasthan is receives rainfall less than 10 cm of annual rainfall (Singh et al. 1974). Thus, rainfall pattern forecasting is necessary for making informed decisions across various sectors. It enhances the ability of governments, communities, and industries to plan and respond effectively to the dynamic and sometimes unpredictable nature of weather patterns, thereby reducing risks and promoting resilience (Zhang et al. 2021, 2023; Lin et al. 2023). Analyzing

rainfall patterns at the state level is highly recommended for effective resource management, and it addresses several challenges associated with this task (Akhter et al. 2017; Liu et al. 2023; Zhou et al. 2023a, b). Therefore, understanding of rainfall distribution patterns is a fundamental step in assessing and managing the risks associated with both floods and droughts (Tarhule 2005; Trenberth 2011; Zho et al. 2022).

Seasonal rainfall knowledge is especially crucial in the context of climate change, where shifts in precipitation patterns can exacerbate the frequency and intensity of both floods and droughts. In essence, understanding the pattern of rainfall distribution is fundamental for making informed decisions in various fields, ranging from water resource management and infrastructure design to climate change adaptation and agricultural planning (Ziervogel et al. 2010; Bhave et al. 2018; Markuna et al. 2023). Rainfall frequency analysis and stochastic modeling are powerful tools that enable researchers and professionals to quantify and predict the complex nature of rainfall patterns (Du and Wang 2014; Gao et al. 2018; Zhao et al. 2022). The rainfall distribution also impacts evapotranspiration processes (Li 2014; Kumar et al. 2016; Kushwaha et al. 2021; Markuna et al. 2023) and groundwater storage which may hamper groundwater quality and increase its remediation cost (Kumar et al. 2013; Asoka et al. 2017; Vishwakarma et al. 2018; Saroughi et al. 2023). Like excess rainfall can cause floods and less rainfall can cause drought. For this reason, accurate rainfall prediction can be helpful in managing these things as well as prevent hydraulic structures to control the floods/drought.

In hydrological modeling, the ANN techniques were applied for the first time by French et al. (1992). Since then, several modeling approaches have been successfully addressed to improve rainfall forecasting models (Ghamariadyan and Imteaz 2021c, b, a; Markuna et al. 2023), rainfall-runoff (Makwana and Tiwari 2014; Asadi et al. 2019; Dumka and Kumar 2021), stream-flow (Chen et al. 2014; Makwana and Tiwari 2017; Shukla et al. 2021; Sammen et al. 2021; Vishwakarma et al. 2023b), sediment discharge (Nourani 2014; Li et al. 2022; Chauhan et al. 2022) water quality (Barzegar et al. 2018; Kumar et al. 2023), ground water (Ch and Mathur 2012; Samantaray et al. 2022; Saroughi et al. 2023), hydraulic conductivity (Sihag 2018; Singh et al. 2019, 2022). In the past, many researchers have studied on rainfall modeling (Zhang and Dong 2001; Tan et al. 2020; Ridwan et al. 2021; Khan et al. 2021). Wu et al. (2010) developed a model that forecasts rainfall on a monthly basis as well as a daily basis. The study demonstrated the applicability of Moving average (MA), Principal Component Analysis (PCA) and Singular Spectral Analysis (SSA) and some forecasting models such as Linear Regression (LR), K-nearest-Neighbors (K-NN),

Artificial Neural Network (ANN) and Modular Artificial Neural Network (MANN) for modelling of monthly rainfall. The results revealed that the SSA technique (singular spectral analysis) was better than moving average (MA) or principal component analysis (PCA) techniques and Modular artificial neural network (MANN) showed a good result on daily rainfall forecasting if MANN was associated with SSA technique. Ridwan et al. (2021) applied four Machine learning models namely Bayesian Linear Regression (BLR), Boosted Decision Tree Regression (BDTR), Decision Forest Regression (DFR) and Neural Network Regression (NNR) for forecasting rainfall in Tasik Kenyir, Terengganu. The BDTR model performed superior to others under the auto correlation function as well as projected error. Khan et al. (2021) performed a comparative study of single decision tree (SDT), tree boost (TB), decision tree forest (DTF), multilayer perceptron (MLP), and gene expression programming (GEP) for rainfall-runoff modelling in the Soan River basin, Pakistan. The study revealed that maximal overlap discrete wavelet transformation (MODWT) based DTF model has high efficacy for Rainfall modelling in the study River basin. Smith et al. (1998) used discrete wavelet transform to detect the characteristic of stream flow and also for detecting its features. Wavelet transform was applied to the daily river discharge (Ahmadi et al. 2022; Pande et al. 2023). The daily river discharge was recorded for 91 rivers in the US. The result obtained from the study suggested that by using the wavelet transform method river flow can be classified into different hydro-climatic categories. Nakken (1999) applied the wavelet theory for identifying the temporal variation in rainfall and runoff and also developing a relationship between them. The Morlet wavelet was used for developing a relationship between rainfall and runoff with respect to time. A dominant frequency was seen since 1950s. Further, Krishna et al. (2011) used the wavelet neural network for developing a time series model for daily river flow of Malaprabha River, Karnataka. The time series was decomposed into a number of sub-series by using discrete wavelet transform. Chen et al. (2014) developed a model for rainfall-runoff simulation by introducing copula entropy (CE) coupled with ANN in the south-western part of China. In this study, for selecting the inputs of ANN model, copula entropy technique was used and three models (Multilayer Feed Forward, Radial biased function, Linear Regression Neural Network) were also used to forecast the stream flow. Study shows that a significant improvement in the forecasting performance of the Jinsha River at Pingshan gauge station when the inputs selected for the copula entropy (CE) method were compared to the inputs chosen for the traditional linear correlation analysis. The MLF ANN model with the inputs selected by the CE method also had the best results. Kang and Lin (2007) used wavelet theory on water quality and hydrological signals for an agricultural

watershed. Three signals based on the precipitation, the water level of wells and streamflow for three periods such as 15 years, hydrologic year and 3 years were taken into consideration. The results suggested that the tool i.e. wavelet transform was found to be useful for analyzing the temporal pattern of the hydrologic as well as for finding out the water quality signals for different scales (temporal scale).

Santos and Freire (2012) analyzed rainfall data from 1901 to 2010 in the northeast region of Brazil consisting of nine states using wavelet transform technique and wavelet spectra approach used to study the variability in monthly rainfall. The results suggested that, a high concentration of rainfall was observed using wavelet spectra technique. Chattopadhyay and Chattopadhyay (2010) developed a uni-variate model to forecast the rainfall data from 1871 to 1999 using Auto-Regressive Integrated Moving Average (ARIMA) and Auto-Regressive Neural Network (ARNN) in India. The study was done for forecasting the summer monsoon and the period of summer monsoon was taken from June to August. Li et al. (2013) examined the atmospheric moisture budget and the regulation of summer precipitation variation over the region of south-east United States during 1948–2007. The inter annual variation in the region was explained using Empirical orthogonal function. Using the wavelet analysis, an increase was identified for 2–4 years in 30 years. The atmospheric moisture budget showed an increasing trend in precipitation because of the moisture transport. Roy et al. (2021) constructed and evaluated an integrated model EO-ELM [Equilibrium Optimizer (EO) and extreme learning machine (ELM)] and a deep neural network (DNN) for rainfall-runoff modelling at two station namely Glanteifi and Fal at Tregony in the UK. The obtained results showed efficient applicability of EO-ELM and DNN in rainfall runoff modelling. Similar attempt was made by Adnan et al. (2021) and compared the performance of ANFIS-PSO, ANFIS-FCM, MARS and M5Tree, together with Multi Model Simple Averaging (MM-SA) for rainfall-runoff modelling on hourly basis. Results shows that ML methods generally performs superior to the EBA4SUB and provides better accuracy than the M5Tree and MARS in some cases.

To the authors knowledge, in literature, no study applied hybrid model of Wavelet-ANN (WANN) for seasonal rainfall modelling in the southern part of Uttarakhand (i.e., namely, Almora, Kashipur, Lansdown and Mukteswar) considered in the present research. Furthermore, the developed methodology, which considers the modelling rainfall employing hybrid algorithm trained on surrounding stations, is in line with practical needs. Therefore, in the present study, a hybrid model using Wavelet-ANN techniques has been developed for predicting the seasonal rainfall in the southern part of Uttarakhand.

2 Material and Methods

2.1 Study Area

Uttarakhand is hilly state of India consisting of 13 districts, having a geographical area of 53,483 km² and it consists of two sub divisions i.e., *Kumaun* and *Garhwal* region. The latitudes and longitudes of Uttarakhand state are 30.066° N and 79.019° E respectively with an elevation ranging from 210 to 7817 m. Four stations of southern district of Uttarakhand has been selected for model development, namely Almora, Mukteswar, Lansdown, Kashipur, and the study area for this work is shown in Fig. 1.

Monthly Rainfall data for the period of 1901 to 2016 was obtained from the Indian metrological department (IMD). Seasonal months were taken according to Indian Metrological department (IMD) and details of data collection for study area were shown in Table 1 and Table 2, respectively. Some basic formulae of statistical parameters have been used in this study and they are listed in Table 3.

Where \bar{x} is the mean of sample size; n is Total number of sample size, SD is standard deviation and x_i is the values in the observation.

2.2 Artificial Neural Network (ANN)

In general, neural network deals with transforming the original signals into meaningful signals. The concept of ANN was introduced by McCulloch and Pitts in 1943 and it is based on biological nervous system (McCulloch and Pitts 1943). In modeling and forecasting of non-linear hydrologic series, Artificial Neural Network has been widely used (Shukla et al. 2021; Elbeltagi et al. 2022a, b; Saroughi et al. 2023). The ANN works on black-box approach, that's why its application does not need any prior information about the techniques (Tzeng and Ma 2005). It is deal in data driven approach and it gives powerful solution of any multifaceted systems. The main characteristic of ANN is that a quick understanding capacity between the input and output signals (Zhang et al. 2017).

In the present study, 'Feed Forward Back Propagation' (FFBP) network has been considered to model the seasonal rainfall data. A FFBP network consisted of three layers viz. Input layer, Hidden layer and Output layer and Levenberg–Marquardt algorithm was used in this study. The training function (TRAINLM) and learning function (LEMRNGDM) were used for calibration the input and output data. Furthermore, there are three types for transfer functions viz. Log sigmoid, Tan sigmoid and purelin function, out of these functions Tansig function was considered as an activation function.

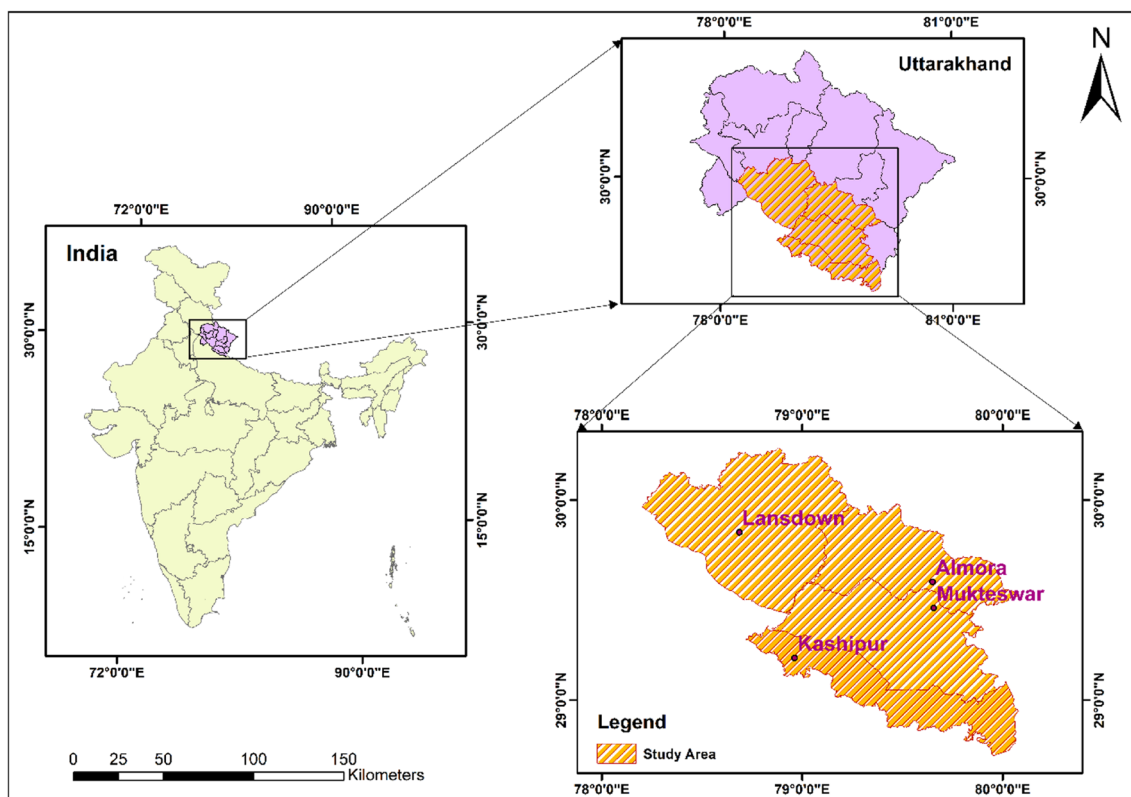


Fig.1 Study area map

Table 1 Seasonal months according to IMD

| Seasons | Months |
|--------------|--------------------|
| Winter | January – February |
| Pre-Monsoon | March – May |
| Monsoon | June – September |
| Post-Monsoon | October – December |

2.3 Wavelet Transform

The Wavelet transform analysis is an advanced technique in signal processing which has gained attention because of theoretical development by Grossmann and Morlet (1984). It is use as an alternative to Fourier transformation and it

is also superior to classical spectral analysis as it allows using different scale for analysing the temporal variations and the main advantage is that the use of stationary series is not required (Smith et al. 1998). Thus, it is appropriate to analyse irregular distributed events and time series that contain non stationary power at many different frequencies. The formula of discrete wavelet transform is given in Eq. (1).

$$\varphi_j^m = a_0^{-m/2} \varphi\left(\frac{y - ja_0^m b_0}{a_0^m}\right) \tag{1}$$

where φ is the Mother wavelet, m is the variable scale, b_0 is Translation Length, j is position unit and a_0 is the base dilation. Furthermore, the continuous form of wavelet transform is described in Eq. (2).

Table 2 Detail of selected area of Uttarakhand, India

| Stations | Altitude (m) (above MSL) | Meridian (Degree) | Parallel (Degree) | Data-Period |
|-----------|--------------------------|-------------------|-------------------|-------------|
| Almora | 1676 | 29.59 N | 79.65 E | 1901–2016 |
| Kashipur | 183 | 29.21 N | 78.95 E | 1901–2016 |
| Lansdown | 1532 | 29.83 N | 78.69 E | 1901–2016 |
| Mukteswar | 2311 | 29.47 N | 78.69 E | 1901–2014 |

Table 3 Statistical parameters used in this study

| | |
|--------------------------------------------|-----------------------------------------------------------|
| Mean | $Mean = \frac{1}{n} \sum_{i=1}^n x_i$ |
| Maximum and Minimum | It is maximum and minimum value calculated in the dataset |
| Standard Deviation (SD) | $SD = \sqrt{\frac{1}{n} \sum_{i=1}^n (x_i - \bar{x})^2}$ |
| Coefficient of Variation (CV) | $CV(\%) = \frac{Standard\ Deviation}{\bar{x}} \times 100$ |
| Coefficient of Skewness (SK _p) | $SK_p = \frac{Mean - Mode}{Standard\ Deviation}$ |

$$WT(b, a) = \frac{1}{\sqrt{a}} \int g\left(\frac{t-b}{a}\right)s(t) \tag{2}$$

where *a* is Scaling Factor; *b* is the time domain; *s(t)* is the signals at time *b*; *g(t)* is the Mother wavelet at ‘*a*’ and ‘*b*’ having value of 0 and 1 respectively.

Although, the use of wavelet is not common in the field of hydrology. It maintains the time and frequencies localization which used in signal analyzing by transforming one-dimensional time series to a diffused two dimensional time–frequency image at the same time, which helps the researcher to get information regarding amplitude of any signal that is periodic within the series and the time varies with respect to time.

The time series of rainfall data for each station has been decomposed using wavelet analysis to get approximate and detailed signal. Thus, using wavelet analysis following relation has been obtained:

$$Rainfall\ time\ series = f(Approximate\ Signal, Detailed\ signal) \tag{3}$$

2.4 Wavelet Artificial Neural Network (WANN) Model

The primary objective of this analysis is to determine the frequency of the signals and the variation in the frequencies that was used for analysis of the data. It provides

information’s related to time, signal frequency and location. It helps to transfer a signal into a set of sub-signal. For the Forecasting of financial time series, WANN model was firstly introduced by Aussem (1998). Wavelet transform analysis is a more appropriate tool than the Fourier transform in studying non-stationary signals (Partial and Kişi 2007). A number of hydrological processes have been developed for wavelet-based hybrid models, which have effectively been applied to studies of water resources with excellent results (Sahay and Srivastava 2014; Seo et al. 2015; Kumar et al. 2015, 2020, 2021; Djerbouai and Souag-Gamane 2016; Araghi et al. 2017; Kisi and Alizamir 2018; Shukla et al. 2021; Drisya et al. 2021; Dumka and Kumar 2021; Bajirao et al. 2021)..

In the present study, Haar wavelet (at level 2) has been used to decompose the seasonal rainfall data. The seasonal rainfall data were decomposed into many sub-signal series to get temporal information about the signal. This sub signals are classified into detailed (d1 and d2) and approximation (A1 and A2) coefficients as described in Fig. 2. Thus,

$$I_a(t)W_a + I_{d1}(t)W_1 + I_{d2}(t)W_2 + I_{d3}(t)W_3 = I(t + 1) \tag{4}$$

where, *W_i* is the weights adjusted by ANN; *I_a(t)* and *I_d(t)* are approximated and detailed signal for rainfall at time *t*; *I(t + 1)* is the rainfall time series one time step ahead of *t*. For determining the neurons in hidden layer, 2N + 1 criteria where N is the number of input neurons has been used (Mishra and Desai 2006).

In order to construct the network architecture, dataset categorized into two portions i.e., 70 percent of total rainfall data were used for training and remaining 30 percent data was used to develop a WANN-model. To compute the level of decomposition Eq. (5) has been used (Nourani et al. 2009).

$$L = int (LogN) \tag{5}$$

where, L is the number of decomposition level and N is the total length of dataset.

The developed models for testing the performance of rainfall prediction is shown in Table 4. The input for these models were the approximated and detailed signals at time

Fig. 2 Schematic diagram of WANN model

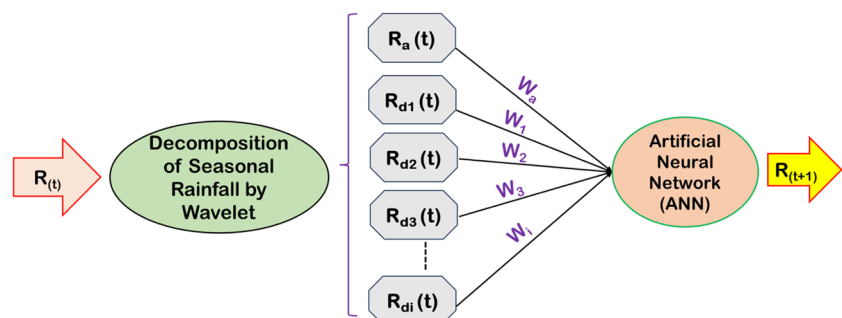


Table 4 Developed WANN Models for rainfall predictions

| Season | Model | Network |
|--------------|---------|---------|
| Monsoon | WANN-01 | 4-6-1 |
| | WANN-02 | 4-7-1 |
| | WANN-03 | 4-8-1 |
| | WANN-04 | 4-9-1 |
| Winter | WANN-05 | 4-6-1 |
| | WANN-06 | 4-7-1 |
| | WANN-07 | 4-8-1 |
| | WANN-08 | 4-9-1 |
| Pre-Monsoon | WANN-09 | 4-6-1 |
| | WANN-10 | 4-7-1 |
| | WANN-11 | 4-8-1 |
| | WANN-12 | 4-9-1 |
| Post-Monsoon | WANN-13 | 4-6-1 |
| | WANN-14 | 4-7-1 |
| | WANN-15 | 4-8-1 |
| | WANN-16 | 4-9-1 |

t (as shown in Eq. 4), and the output was the signal at one time ahead signal.

2.5 Evaluating Criteria for Model Performance

Wavelet Artificial Neural Network models were evaluated using performance indexes, and the model network with the best performance was selected for use in the simulation of rainfall-runoff based on the WANN model with the best performance index. For evaluating the performance of designed model, Root Mean Square Error (RMSE), coefficient of determination (R^2) and coefficient of efficiency (CE) have been selected whose equation is stated from Eqs. 6–8.

$$RMSE = \left(\frac{1}{n} (O_i - P_i) \right)^{0.5} \quad (0 < RMSE < \infty) \quad (6)$$

$$CE = 1 - \left(\frac{\sum_{i=1}^N (O_i - P_i)^2}{\sum_{i=1}^N (P_i - \bar{P})^2} \right) \quad (-\infty < COE < 1) \quad (7)$$

$$R^2 = \left(\frac{\sum_{i=1}^N (O_i - \bar{O})(P_i - \bar{P})}{\left(\sqrt{\left(\sum_{i=1}^N (O_i - \bar{O})^2 \right) \left(\sum_{i=1}^N (P_i - \bar{P})^2 \right)} \right)} \right)^2 \quad (0 < R^2 < 1) \quad (8)$$

where O_i is the observed rainfall and P_i is the predicted rainfall for the i^{th} time-series; n is the total length of time-series;

\bar{P} and \bar{O} are indicating the average value of observed and predicted rainfall respectively.

R^2 is an index of the degree of linear relationship between observed and predicted data. CE is a measure of how well the plot between the observed values and the predicted values fits the 1:1 line when plotted against the observed values. The model performance must be evaluated based on at least one absolute error measure (e.g. RMSE) to ensure that the model is as accurate as possible. Those models having least RMSE and CE and R^2 value close to 1, the model will be considered as best and superior model (Saroughi et al. 2023; Vishwakarma et al. 2023a, b; Mirzania et al. 2023; Kumar et al. 2023).

3 Results

3.1 Statistical Analysis of Seasonal Rainfall

The long-term rainfall statistics of Almora, Lansdown and Kashipur and Mukteshwar is shown in Tables 5 to 8. It can be depicted that at Almora, lowest and highest seasonal rainfall was found to be zero and 1187.20 mm respectively (Table 5). At Lansdown station, the highest value of rainfall i.e., 2826.70 mm and lowest rainfall i.e., zero was measured (Table 6). At Kashipur station, the mean rainfall varied from 48.45 mm to 1060.53 mm and maximum rainfall

Table 5 Statistical analysis of seasonal rainfall (mm) data for Almora

| Statistical parameter | Winter | Pre- monsoon | Monsoon | Post-monsoon |
|-----------------------|--------|--------------|---------|--------------|
| Mean (mm) | 91.05 | 112.42 | 746.82 | 60.40 |
| Maximum (mm) | 320.60 | 270.40 | 1187.20 | 374.50 |
| Minimum (mm) | 5.80 | 0.00 | 284.80 | 0.00 |
| SD (mm) | 57.05 | 59.27 | 185.58 | 65.56 |
| CV (%) | 62.66 | 52.72 | 24.85 | 108.54 |
| CS | 1.32 | 0.62 | 0.34 | 2.54 |

Table 6 Statistical analysis of seasonal rainfall (mm) data for Lansdown

| Statistical parameter | Winter | Pre-monsoon | Monsoon | Post-monsoon |
|-----------------------|--------|-------------|---------|--------------|
| Mean (mm) | 118.48 | 115.48 | 1586.58 | 75.60 |
| Maximum | 464.20 | 440.30 | 2826.70 | 540.80 |
| Minimum | 0.00 | 0.00 | 0.00 | 0.00 |
| SD (mm) | 95.94 | 81.59 | 519.00 | 103.82 |
| CV (%) | 80.98 | 70.65 | 32.71 | 137.33 |
| CS | 1.08 | 1.12 | -0.06 | 2.67 |

was measured for the monsoon season i.e., 2716.40 mm among all the seasons whereas lowest rainfall was found zero in all the seasons except monsoon season (Table 7). At Mukteswar station, the mean rainfall varied from 85.04 mm to 964.43 mm and minimum value of rainfall was found zero in post-monsoon season. The maximum, SD, CV and SC of seasonal rainfall data ranged from 336.90 mm to 1839 mm, 65.34 mm to 256.22 mm, 26.57% to 111.34% and 0.65 to 2.29 respectively (Table 8).

Pimentel-Gomes (2023) classified the CV as follows: Low: Lower than 10%; Average: 10–20%; High: 20–30%; Very high: Higher than 30%. The result shown in Tables 5, 6, 7 and 8, and the visual interpretation in Fig. 3, describethe level of variability and found very high in all station except Almora and Mukteswar in mansoon season.

3.2 Forecasting Seasonal Rainfall Using WANN-Model

3.2.1 Model selection

The developed model has been selected based on training results with the help of low value of Root Mean Square Error (RMSE), high value of coefficient of determination (R^2) and coefficient of efficiency (CE). The training, testing and overall value of R^2 of seasonal rainfall were conducted for the selected stations namely Kashipur, Lansdown, Almora and

Table 7 Statistical analysis of seasonal rainfall (mm) data for Kashipur

| Statistical param- eter | Winter | Pre-monsoon | Monsoon | Post-monsoon |
|----------------------------|--------|-------------|---------|--------------|
| Mean (mm) | 62.51 | 48.45 | 1060.53 | 59.50 |
| Maximum (mm) | 248.40 | 208.30 | 2716.40 | 451.90 |
| Minimum (mm) | 0.00 | 0.00 | 212.00 | 0.00 |
| SD (mm) | 53.86 | 40.47 | 456.87 | 83.95 |
| CV (%) | 86.15 | 83.52 | 43.08 | 141.10 |
| CS | 1.07 | 1.16 | 1.05 | 2.43 |

Table 8 Statistical analysis of seasonal rainfall (mm) data for Mukteswar

| Statistical param- eter | Winter | Pre-monsoon | Monsoon | Post-monsoon |
|----------------------------|--------|-------------|---------|--------------|
| Mean (mm) | 112.25 | 147.93 | 964.43 | 85.04 |
| Maximum (mm) | 336.90 | 376.00 | 1839.00 | 478.90 |
| Minimum (mm) | 2.80 | 18.80 | 467.10 | 0.00 |
| SD (mm) | 65.34 | 71.80 | 256.22 | 94.68 |
| CV (%) | 58.21 | 48.53 | 26.57 | 111.34 |
| CS | 0.88 | 0.82 | 0.65 | 2.29 |

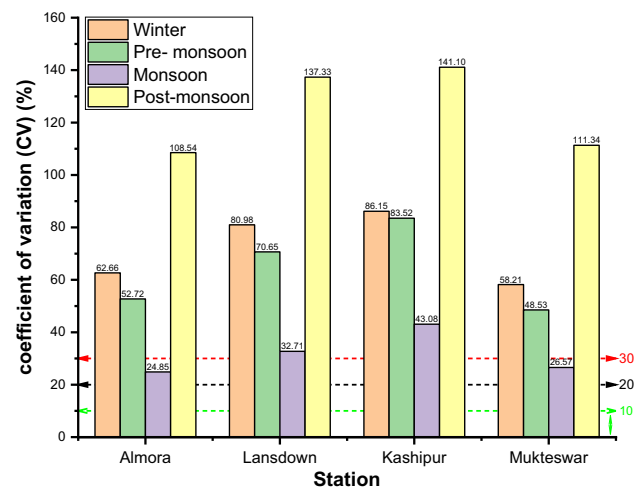


Fig. 3 Variability of rainfall atAlmora, Lansdown and Kashipur and Mukteswar

Mukteswar. Furthermore, four networks of WANN model for each seasons were designed by varying the numbers of neurons in the Hidden layer and based of model performance, one WANN model has been finalized out of total designed models.

3.2.2 WANN-model for Lansdown station

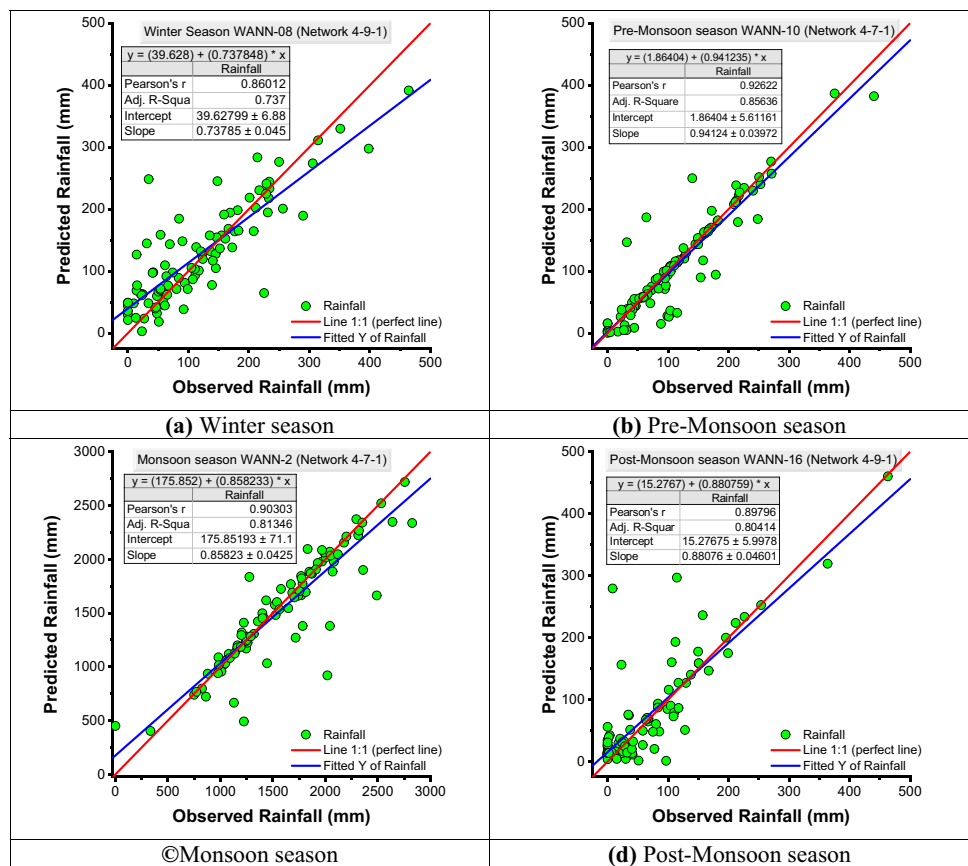
The prediction accuracy of the different WANN models during the training, testing and overall data sets for Lansdown stationare illustrated in Table 9. The result shows overall R^2 , RMSE (mm/month) and CE values ranging from 0.665 to 0.857 (mean = 0.744), 32.192 to 303.682 mm/month (mean = 106.437 mm/month), and 0.636 to 0.846 (mean = 0.722) for the Lansdown station. For the monsoon season, WANN-02 (4–7-1 Network) model performed superior than the other designed network. The overall measured value of R^2 , RMSE and CE were found 0.815, 232.736 mm/month and 0.805 respectively. Out of four designed network, WANN-08 (Network 4–9-1) found best for the winter season under the criteria of overall highest value of coefficient of determination and CE ($R^2=0.740$, $CE=0.732$), lowest value of RMSE (49.073 mm/month) (Table 9). Similarly, for the pre-monsoon season, the WANN-10 (4–7-1 Network) model was found superior as the its achieved highest value of R^2 and CE i.e., 0.857 and 0.846 respectively, and lowest value of RMSE i.e., 32.192 mm/month out of four designed network of pre-monsoon season. In the same way, the post-monsoon season, WANN-16 (Network, 4–9-1) model performed superior than the other designed network. The overall measured value of R^2 , RMSE and CE were found 0.806, 47.739 mm/month and 0.796 respectively (Table 9).

Furthermore, the scattered plot of observed rainfall versus predicted rainfall is shown in Fig. 4 for all seasons. Model

Table 9 Selected models of all the seasons for Lansdown station

| Season | Model | Network | Training | Testing | Overall | | |
|--------------|---------|--------------|----------------|----------------|----------------|----------------|--------------|
| | | | R ² | R ² | R ² | RMSE | CE |
| Monsoon | WANN-01 | 4-6-1 | 0.750 | 0.291 | 0.674 | 301.484 | 0.672 |
| | WANN-02 | 4-7-1 | 0.988 | 0.361 | 0.815 | 232.736 | 0.805 |
| | WANN-03 | 4-8-1 | 0.799 | 0.678 | 0.750 | 273.747 | 0.730 |
| | WANN-04 | 4-9-1 | 0.745 | 0.661 | 0.669 | 303.682 | 0.667 |
| Winter | WANN-05 | 4-6-1 | 0.803 | 0.282 | 0.718 | 50.864 | 0.712 |
| | WANN-06 | 4-7-1 | 0.908 | 0.584 | 0.665 | 57.188 | 0.636 |
| | WANN-07 | 4-8-1 | 0.852 | 0.757 | 0.713 | 56.445 | 0.645 |
| | WANN-08 | 4-9-1 | 0.870 | 0.557 | 0.740 | 49.073 | 0.732 |
| Pre-Monsoon | WANN-09 | 4-6-1 | 0.790 | 0.591 | 0.752 | 41.468 | 0.743 |
| | WANN-10 | 4-7-1 | 0.988 | 0.572 | 0.857 | 32.192 | 0.846 |
| | WANN-11 | 4-8-1 | 0.837 | 0.669 | 0.765 | 43.569 | 0.718 |
| Post-Monsoon | WANN-12 | 4-9-1 | 0.806 | 0.421 | 0.721 | 46.016 | 0.686 |
| | WANN-13 | 4-6-1 | 0.916 | 0.391 | 0.776 | 50.275 | 0.771 |
| | WANN-14 | 4-7-1 | 0.962 | 0.558 | 0.774 | 57.074 | 0.705 |
| | WANN-15 | 4-8-1 | 0.723 | 0.736 | 0.701 | 59.432 | 0.680 |
| | WANN-16 | 4-9-1 | 0.893 | 0.692 | 0.806 | 47.739 | 0.796 |

Fig. 4 Scatter plot between observed and predicted rainfall for Lansdown station



WANN-10 (4-7-1 Network), based on the WANN algorithm and seasonal comparison, achieved the best overall performance in predicting the rainfall for Lansdown station data set. WANN-10 (4-7-1 Network) achieved the best R², RMSE

and CE values with scores 0.857, 32.192 mm/month and 0.846 respectively, hence giving it the highest accuracy as the observed values are very closed to line 1:1 pre-monsoon season.

3.2.3 WANN-model for Almora station

The prediction accuracy of the different WANN models during the training, testing and overall data sets for Almora station are illustrated in Table 10. The result shows overall R^2 , RMSE (mm/month) and CE values ranging from 0.684 to 0.822 (mean = 0.735), 24.804 to 96.906 mm/month (mean = 47.512 mm/month), and 0.680 to 0.810 (mean = 0.726) for the Almora station. For the monsoon season, WANN-02 (4–7-1 Network) model performed superior than the other designed network. The overall measured value of R^2 , RMSE and CE were found 0.781, 88.011 mm/month and 0.776 respectively. Out of four designed network, WANN-08 (Network 4–9-1) found best for the winter season under the criteria of overall highest value of coefficient of determination and CE ($R^2 = 0.822$, $CE = 0.810$), lowest value of RMSE (24.804 mm/month) (Table 10). Similarly, for the pre-monsoon season, the WANN-9 (4–6-1 Network) model was found superior as the its achieved highest value of R^2 and CE i.e., 0.704 and 0.701 respectively, and lowest value of RMSE i.e., 32.865 mm/month out of four designed network of pre-monsoon season. In the same way, the post-monsoon season, WANN-15 (Network, 4–8-1) model performed superior than the other designed network. The overall measured value of R^2 , RMSE and CE were found 0.732, 34.771 mm/month and 0.725 respectively (Table 10).

Furthermore, the scattered plot of observed rainfall versus predicted rainfall is shown in Fig. 5 for all seasons. Model WANN-8 (4–9-1 Network), based on the WANN algorithm and seasonal comparison, achieved the best overall performance in predicting the rainfall for Almora station data set. WANN-8 (4–9-1 Network) achieved the best R^2 , RMSE and

CE values with scores 0.822, 24.804 mm/month and 0.810 respectively, hence giving it the highest accuracy as the observed values are very closed to line 1:1 for winter season.

3.2.4 WANN-model for Mukteswar station

The prediction accuracy of the different WANN models during the training, testing and overall data sets for Mukteswar station are illustrated in Table 11. The result shows overall R^2 , RMSE (mm/month) and CE values ranging from 0.661 to 0.867 (mean = 0.745), 32.575 to 134.340 mm/month (mean = 61.380 mm/month), and 0.566 to 0.864 (mean = 0.732) for the Mukteswar station. For the monsoon season, WANN-03 (4–8-1 Network) model performed superior than the other designed network. The overall measured value of R^2 , RMSE and CE were found 0.867, 94.317 mm/month and 0.864 respectively. Out of four designed network, WANN-05 (Network 4–6-1) found best for the winter season under the criteria of overall highest value of coefficient of determination and CE ($R^2 = 0.748$, $CE = 0.748$), lowest value of RMSE (32.575 mm/month) (Table 11). Similarly, for the pre-monsoon season, the WANN-10 (4–7-1 Network) model was found superior as the its achieved highest value of R^2 and CE i.e., 0.780 and 0.738 respectively, and lowest value of RMSE i.e., 37.232 mm/month out of four designed network of pre-monsoon season. In the same way, the post-monsoon season, WANN-16 (Network, 4–9-1) model performed superior than the other designed network. The overall measured value of R^2 , RMSE and CE were found 0.817, 41.631 mm/month and 0.811 respectively (Table 11).

Furthermore, the scattered plot of observed rainfall versus predicted rainfall is shown in Fig. 6 for all seasons. Model

Table 10 Models of all the seasons for Almora station

| Season | Model | Network | Training | Testing | Overall | | |
|--------------|---------|--------------|--------------|--------------|--------------|---------------|--------------|
| | | | R^2 | R^2 | R^2 | RMSE | CE |
| Monsoon | WANN-01 | 4–6-1 | 0.783 | 0.590 | 0.731 | 96.906 | 0.728 |
| | WANN-02 | 4-7-1 | 0.897 | 0.373 | 0.781 | 88.011 | 0.776 |
| | WANN-03 | 4–8-1 | 0.822 | 0.611 | 0.762 | 90.838 | 0.761 |
| | WANN-04 | 4–9-1 | 0.773 | 0.458 | 0.736 | 95.373 | 0.736 |
| Winter | WANN-05 | 4–6-1 | 0.837 | 0.326 | 0.729 | 29.605 | 0.729 |
| | WANN-06 | 4–7-1 | 0.745 | 0.433 | 0.684 | 31.966 | 0.684 |
| | WANN-07 | 4–8-1 | 0.771 | 0.740 | 0.774 | 26.973 | 0.775 |
| | WANN-08 | 4-9-1 | 0.874 | 0.456 | 0.822 | 24.804 | 0.810 |
| Pre-Monsoon | WANN-09 | 4-6-1 | 0.757 | 0.581 | 0.704 | 32.865 | 0.701 |
| | WANN-10 | 4–7-1 | 0.748 | 0.702 | 0.706 | 33.094 | 0.697 |
| | WANN-11 | 4–8-1 | 0.974 | 0.263 | 0.722 | 33.072 | 0.697 |
| | WANN-12 | 4–9-1 | 0.769 | 0.723 | 0.706 | 33.447 | 0.690 |
| Post-Monsoon | WANN-13 | 4–6-1 | 0.962 | 0.125 | 0.719 | 35.748 | 0.710 |
| | WANN-14 | 4–7-1 | 0.790 | 0.643 | 0.739 | 35.208 | 0.718 |
| | WANN-15 | 4-8-1 | 0.999 | 0.508 | 0.732 | 34.771 | 0.725 |
| | WANN-16 | 4–9-1 | 0.924 | 0.145 | 0.711 | 37.512 | 0.680 |

Fig. 5 Scatter plot between observed and predicted rainfall for Almora station

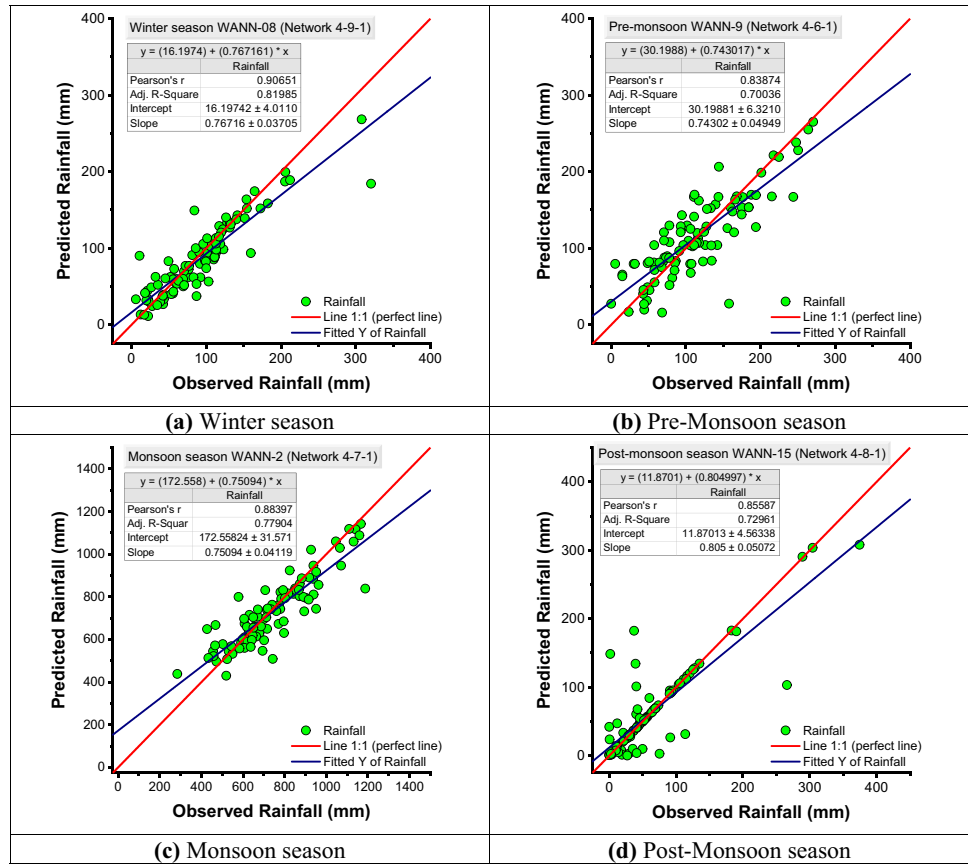


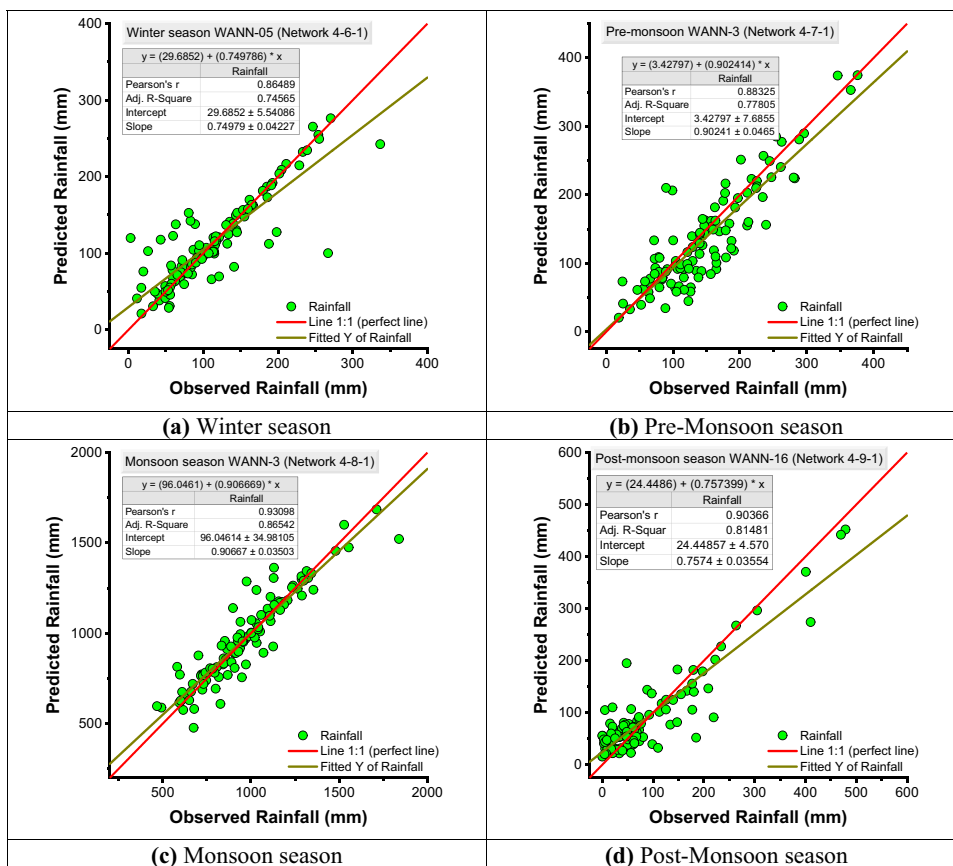
Table 11 Selected models of all the seasons for Mukteswar station

| Season | Model | Network | Training R ² | Testing R ² | Overall | | |
|--------------|---------|--------------|-------------------------|------------------------|----------------|---------------|--------------|
| | | | | | R ² | RMSE | CE |
| Monsoon | WANN-01 | 4-6-1 | 0.889 | 0.346 | 0.728 | 134.340 | 0.725 |
| | WANN-02 | 4-7-1 | 0.821 | 0.567 | 0.738 | 131.384 | 0.737 |
| | WANN-03 | 4-8-1 | 0.953 | 0.701 | 0.867 | 94.317 | 0.864 |
| | WANN-04 | 4-9-1 | 0.781 | 0.539 | 0.750 | 131.156 | 0.738 |
| Winter | WANN-05 | 4-6-1 | 0.801 | 0.769 | 0.748 | 32.575 | 0.748 |
| | WANN-06 | 4-7-1 | 0.824 | 0.516 | 0.731 | 33.958 | 0.726 |
| | WANN-07 | 4-8-1 | 0.835 | 0.433 | 0.687 | 36.965 | 0.675 |
| | WANN-08 | 4-9-1 | 0.839 | 0.594 | 0.748 | 32.781 | 0.745 |
| Pre-Monsoon | WANN-09 | 4-6-1 | 0.771 | 0.428 | 0.716 | 39.398 | 0.707 |
| | WANN-10 | 4-7-1 | 0.854 | 0.630 | 0.780 | 37.232 | 0.738 |
| | WANN-11 | 4-8-1 | 0.856 | 0.658 | 0.726 | 38.208 | 0.724 |
| | WANN-12 | 4-9-1 | 0.803 | 0.381 | 0.728 | 38.038 | 0.726 |
| Post-Monsoon | WANN-13 | 4-6-1 | 0.823 | 0.621 | 0.766 | 46.708 | 0.762 |
| | WANN-14 | 4-7-1 | 0.834 | 0.517 | 0.661 | 63.080 | 0.566 |
| | WANN-15 | 4-8-1 | 0.790 | 0.300 | 0.729 | 50.307 | 0.724 |
| | WANN-16 | 4-9-1 | 0.893 | 0.642 | 0.817 | 41.631 | 0.811 |

WANN-3 (4-8-1 Network), based on the WANN algorithm and seasonal comparison, achieved the best overall performance in predicting the rainfall for Mukteswar station data set. WANN-3 (4-8-1 Network) achieved the best R², RMSE

and CE values with scores 0.867, 94.317 mm/month and 0.864 respectively, hence giving it the highest accuracy as the observed values are very closed to line 1:1 for winter season.

Fig. 6 Scatter plot between observed and predicted rainfall for Mukteswar station



3.2.5 WANN-model for Kashipur station

The prediction accuracy of the different WANN models during the training, testing and overall data sets for Kashipur

station are illustrated in Table 12. The result shows overall R^2 , RMSE (mm/month) and CE values ranging from 0.700 to 0.998 (mean = 0.808), 1.240 to 269.357 mm/month (mean = 81.338 mm/month), and 0.660 to 0.999

Table 12 Selected models of all the seasons for Kashipur station

| Season | Model | Network | Training | Testing | Overall | | |
|--------------|---------|---------|--------------|--------------|--------------|----------------|--------------|
| | | | R^2 | R^2 | R^2 | RMSE | CE |
| Monsoon | WANN-01 | 4-6-1 | 0.982 | 0.142 | 0.771 | 239.490 | 0.731 |
| | WANN-02 | 4-7-1 | 0.707 | 0.588 | 0.719 | 249.966 | 0.707 |
| | WANN-03 | 4-8-1 | 0.767 | 0.278 | 0.710 | 249.282 | 0.709 |
| | WANN-04 | 4-9-1 | 0.960 | 0.442 | 0.733 | 269.357 | 0.660 |
| Winter | WANN-05 | 4-6-1 | 0.747 | 0.158 | 0.700 | 29.358 | 0.695 |
| | WANN-06 | 4-7-1 | 0.935 | 0.293 | 0.712 | 28.802 | 0.706 |
| | WANN-07 | 4-8-1 | 0.819 | 0.677 | 0.737 | 27.500 | 0.732 |
| | WANN-08 | 4-9-1 | 0.833 | 0.622 | 0.786 | 24.785 | 0.782 |
| Pre-Monsoon | WANN-09 | 4-6-1 | 1.000 | 0.983 | 0.994 | 3.343 | 0.993 |
| | WANN-10 | 4-7-1 | 0.999 | 0.996 | 0.998 | 1.240 | 0.999 |
| | WANN-11 | 4-8-1 | 1.000 | 0.989 | 0.994 | 2.735 | 0.995 |
| | WANN-12 | 4-9-1 | 1.000 | 0.932 | 0.966 | 8.104 | 0.959 |
| Post-Monsoon | WANN-13 | 4-6-1 | 0.800 | 0.797 | 0.752 | 43.846 | 0.735 |
| | WANN-14 | 4-7-1 | 0.758 | 0.674 | 0.764 | 43.435 | 0.740 |
| | WANN-15 | 4-8-1 | 0.996 | 0.724 | 0.865 | 34.118 | 0.839 |
| | WANN-16 | 4-9-1 | 0.837 | 0.669 | 0.732 | 46.050 | 0.707 |

(mean = 0.793) for the Kashipur station. For the monsoon season, WANN-01 (4–6–1 Network) model performed superior than the other designed network. The overall measured value of R^2 , RMSE and CE were found 0.771, 239.490 mm/month and 0.731 respectively. Out of four designed network, WANN-08 (Network 4–9–1) found best for the winter season under the criteria of overall highest value of coefficient of determination and CE ($R^2=0.786$, $CE=0.782$), lowest value of RMSE (24.785 mm/month) (Table 12). Similarly, for the pre-monsoon season, the WANN-10 (4–7–1 Network) model was found superior as the its achieved highest value of R^2 and CE i.e., 0.998 and 0.999 respectively, and lowest value of RMSE i.e., 1.240 mm/month out of four designed network of pre-monsoon season. In the same way, the post-monsoon season, WANN-15 (Network, 4–8–1) model performed superior than the other designed network. The overall measured value of R^2 , RMSE and CE were found 0.865, 34.118 mm/month and 0.839 respectively (Table 12).

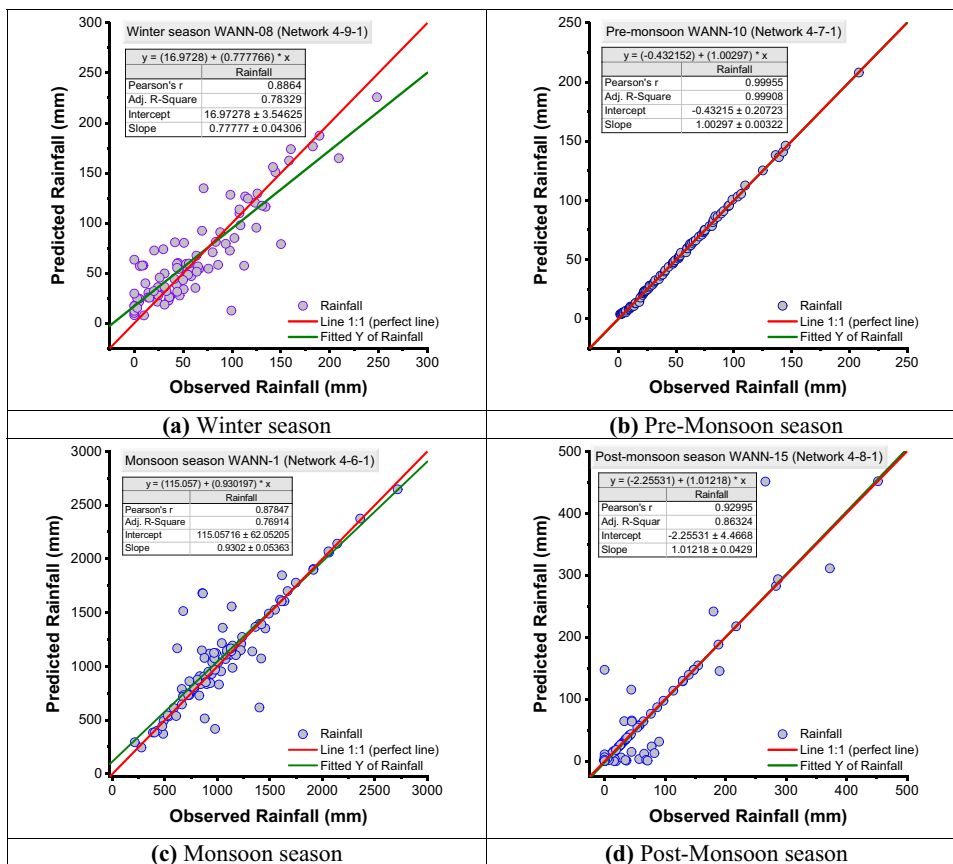
Furthermore, the scattered plot of observed rainfall versus predicted rainfall is shown in Fig. 7 for all seasons. Model WANN-10 (4–7–1 Network), based on the WANN algorithm and seasonal comparison, achieved the best overall performance in predicting the rainfall for Kashipur station data set. WANN-10 (4–7–1 Network) achieved the best R^2 , RMSE and CE values with scores 0.998, 1.240 mm/month

and 0.999 respectively, hence giving it the highest accuracy as the observed values are very closed to line 1:1 for winter season. One interesting thing also noticed for the Kashipur station that performance of all models in training was so higher than all the stations.

4 Discussion

Because of the geographical location of Uttarakhand, the Almora, Kashipur, Lansdown, and Mukteswar climate index has a stronger impact on rainfall variability in this region. In spite of the fact that climate drivers interact with rainfall in complex ways, sometimes it is impossible to predict rainfall with a high level of accuracy in response to an individual climate driver alone because of the complex relationships between them. A total of 16 different models (WANN-01 to WANN-16) were selected to compare the effect of climate indices on Uttarakhand rainfall on a monthly basis in this study. In the present study, the desecrate wavelet transform coupled with ANN was employed to significantly enhance the accuracy of the seasonal rainfall prediction. Considering all four regions considered, it is evident that the performances of the WANN-03 (Network 4–8–1), WANN-10 model (Network 4–7–1), WANN-10 (Network 4–7–1) and

Fig. 7 Scatter plot between observed and predicted rainfall for Kashipur station



WANN-15 (Network 4–8-1) models when considering the R^2 , RMSE, and CE values for the Mukteswar, Lansdown, Kashipur and Almora regions respectively, are considerably better than the performances of the other WANN models. The results from this study have demonstrated that the introduction of easily estimated input variables into WNN models is a very useful tool for improving precipitation predictions, especially when there are no long-term datasets available that can provide a good estimation of future precipitation amounts. These wavelet models coupled with ANN performed better when prediction of rainfall (Ray et al. 2020; Ghamariadyan and Imteaz 2021c; Tiwari et al. 2023) and while other studies simulate stream flow using specific algorithms which is based on ANN such as LM, SDG and BR-ANN (Rautela et al. 2022). In addition, our results showed lower RMSE values than those reported by Jiang and Wu (2013) in a study of ten stations in Guilin (China), using evolutionary models to estimate the RMSE values. Considering the efficiency of the models, the mean CE values indicate that they all have good levels of efficiency, and they are significantly higher than the values reported by Kalteh (2017) in Iran, which used ANNs to predict monthly precipitation using 30-year series to conduct the study. Before being utilized as an input to the ANN, the discrete signals (representing seasonal rainfall) were first decomposed into smaller signals, and then used as input. During analysis, some models perform very well when the number of neurons in the hidden layer is less, or some models perform badly even though the number of neurons in the hidden layer is high (Zhang and Morris 1998; Ke and Liu 2008; Sheela and Deepa 2013; Shukla et al. 2021; Rachmatullah et al. 2021). Therefore, it is recommended that the relationship between the hidden layer neuron and the best-performing model be context-specific and may also depend on the larger dataset. The local farmers and policymakers in the studied regions may find this study valuable in mitigating issues associated with water. The future scope of this study is as follows: In this research, the number of rain gauge stations is limited due to data availability. Consequently, it is recommended that future studies expand by including a greater number of stations. Additionally, the prediction of rainfall could be extended to various time scales, encompassing seasons such as daily and monthly intervals. Furthermore, it is advised to integrate diverse models employing remote sensing and deep learning approaches.

5 Conclusion

In the present study, four stations of Uttarakhand state namely, Almora, Kashipur Lansdown, and Mukteswar were taken into consideration for analyzing the statistical parameters and also to develop a hybrid WANN model. These

stations were selected on the basis of data availability. Six statistical parameters such as mean, maximum, minimum, coefficient of variation, coefficient of skewness and standard deviation were employed for analyzing the seasonal rainfall data. A hybrid model of Wavelet coupled with ANN was developed to model seasonal rainfall. For evaluating the performance of the designed model Root Mean Square Error (RMSE), Coefficient of determination (R^2) and Coefficient of Efficiency (CE) were used. The highest mean rainfall was observed in the winter season for the Lansdown station. Lansdowne station received the highest rainfall compared to all the stations. In the analysis based on pre-monsoon and post-monsoon reading, Mukteswar holds the highest value of mean rainfall. Similarly, for monsoon, Lansdownwaste highest value. The maximum rainfall for pre-monsoon, post monsoon, and winter in the southwest monsoon was seen in the Lansdown region. For Mukteswar, Lansdown, Kashipur and Almora, the model WANN-03 (Network 4–8-1), WANN-10 model (Network 4–7-1), WANN-10 (Network 4–7-1) and WANN-15 (Network 4–8-1), respectively were found to be most efficient model as the R^2 value was high and the RMSE obtained was low. The overall value for R^2 was found high in these models. The selection of these models for the particular region was based on comparisons between the models and their seasons. Among all the stations investigated in the study, the hybrid model of WANN-10 with a Network (4–7-1) was found to be the most superior model for the Lansdown stations out of all those investigated.

Acknowledgements Authors are thankful to India Meteorological Department, Pune, India for providing the necessary rainfall data for research work.

Author contribution Conceptualization: Shekhar Singh, Deepak kumar; Methodology: Shekhar Singh; Formal analysis and investigation: Shekhar Singh and Dinesh Kumar Vishwakarma; Software: Shekhar Singh, Deepak kumar; Visualization: Shekhar Singh and Dinesh Kumar Vishwakarma; Writing – original draft preparation: Shekhar Singh, Dinesh Kumar Vishwakarma, Rohitashw Kumar and Nand Lal Kushwaha; Writing – review and editing: Dinesh Kumar Vishwakarma, Rohitashw Kumar; Resources: Deepak kumar; Supervision: Deepak kumar and Dinesh Kumar Vishwakarma.

Funding The authors declare that no funds, grants, or other support were received during the preparation of this manuscript.

Data availability The datasets analysed during the current study are not publicly available due to policy of data providing agency but are available from the corresponding author on reasonable request.

Code availability Not applicable.

Declarations

Ethics approval Not applicable.

Consent to participate The authors express their consent to participate in research and review.

Consent for publication The authors express their consent for publication of research work.

Conflict of interest The authors declare no competing interests.

References

- Adnan RM, Petroselli A, Heddad S et al (2021) Short term rainfall-runoff modelling using several machine learning methods and a conceptual event-based model. *Stoch Environ Res Risk Assess* 35:597–616. <https://doi.org/10.1007/s00477-020-01910-0>
- Ahmadi F, Mirabbasi R, Gajbhiye S, Kumar R (2022) Investigating the variation pattern and erosivity power of precipitation in the Sidh River Basin of India during last 120 years. *Stoch Environ Res Risk Assess* 36:3265–3279. <https://doi.org/10.1007/s00477-022-02193-3>
- Akhter J, Das L, Deb A (2017) CMIP5 ensemble-based spatial rainfall projection over homogeneous zones of India. *Clim Dyn* 49:1885–1916. <https://doi.org/10.1007/s00382-016-3409-8>
- Araghi A, Mousavi-Baygi M, Adamowski J et al (2017) Forecasting soil temperature based on surface air temperature using a wavelet artificial neural network. *Meteorol Appl* 24:603–611. <https://doi.org/10.1002/met.1661>
- Asadi H, Shahedi K, Jarihani B, Sidle RC (2019) Rainfall-Runoff Modelling Using Hydrological Connectivity Index and Artificial Neural Network Approach. *Water* 11:212
- Asoka A, Gleeson T, Wada Y, Mishra V (2017) Relative contribution of monsoon precipitation and pumping to changes in groundwater storage in India. *Nat Geosci* 10:109–117. <https://doi.org/10.1038/ngeo2869>
- Aussem A (1998) Waveletbased feature extraction and decomposition strategies for financial forecasting. *Int J Comput Intell Financ* 6:5–12
- Bajirao TS, Kumar P, Kumar M et al (2021) Potential of hybrid wavelet-coupled data-driven-based algorithms for daily runoff prediction in complex river basins. *Theor Appl Climatol* 145:1207–1231. <https://doi.org/10.1007/s00704-021-03681-2>
- Barzegar R, AsghariMoghaddam A, Adamowski J, Ozga-Zielinski B (2018) Multi-step water quality forecasting using a boosting ensemble multi-wavelet extreme learning machine model. *Stoch Environ Res Risk Assess* 32:799–813. <https://doi.org/10.1007/s00477-017-1394-z>
- Bhave AG, Conway D, Dessai S, Stainforth DA (2018) Water Resource Planning Under Future Climate and Socioeconomic Uncertainty in the Cauvery River Basin in Karnataka, India. *Water Resour Res* 54:708–728. <https://doi.org/10.1002/2017WR020970>
- Ch S, Mathur S (2012) Groundwater level forecasting using SVM-PSO. *Int J Hydrol Sci Technol* 2:202. <https://doi.org/10.1504/IJHST.2012.047432>
- Chattopadhyay S, Chattopadhyay G (2010) Univariate modelling of summer-monsoon rainfall time series: Comparison between ARIMA and ARNN. *Comptes Rendus Geosci* 342:100–107. <https://doi.org/10.1016/j.crte.2009.10.016>
- Chauhan P, Akiner ME, Sain K, Kumar A (2022) Forecasting of suspended sediment concentration in the Pindari-Kafni glacier valley in Central Himalayan region considering the impact of precipitation: using soft computing approach. *Arab J Geosci* 15:683. <https://doi.org/10.1007/s12517-022-09773-1>
- Chen L, Singh VP, Guo S et al (2014) Copula entropy coupled with artificial neural network for rainfall-runoff simulation. *Stoch Environ Res Risk Assess* 28:1755–1767. <https://doi.org/10.1007/s00477-013-0838-3>
- Djerbouai S, Souag-Gamane D (2016) Drought Forecasting Using Neural Networks, Wavelet Neural Networks, and Stochastic Models: Case of the Algerois Basin in North Algeria. *Water Resour Manag* 30:2445–2464. <https://doi.org/10.1007/s11269-016-1298-6>
- Drisya J, Kumar DS, Roshni T (2021) Hydrological drought assessment through streamflow forecasting using wavelet enabled artificial neural networks. *Environ Dev Sustain* 23:3653–3672. <https://doi.org/10.1007/s10668-020-00737-7>
- Du W, Wang G (2014) Fully probabilistic seismic displacement analysis of spatially distributed slopes using spatially correlated vector intensity measures. *Earthquake Eng Struct Dynam* 43(5):661–679. <https://doi.org/10.1002/eqe.2365>
- Dumka BB, Kumar P (2021) Modeling rainfall-runoff using Artificial Neural Network (ANNs) and Wavelet based ANNs (WANNs) for Haripura Dam, Uttarakhand. *Indian J Ecol* 48:271–274
- Elbeltagi A, Kushwaha NL, Rajput J et al (2022b) Modelling daily reference evapotranspiration based on stacking hybridization of ANN with meta-heuristic algorithms under diverse agroclimatic conditions. *Stoch Environ Res Risk Assess* 36:3311–3334. <https://doi.org/10.1007/s00477-022-02196-0>
- Elbeltagi A, Kushwaha NL, Rajput J et al (2022a) Modelling daily reference evapotranspiration based on stacking hybridization of ANN with meta-heuristic algorithms under diverse agroclimatic conditions. *Stoch Environ Res Risk Assess* 36:3311–3334. <https://doi.org/10.1007/s00477-022-02196-0>
- French MN, Krajewski WF, Cuykendall RR (1992) Rainfall forecasting in space and time using a neural network. *J Hydrol* 137:1–31. [https://doi.org/10.1016/0022-1694\(92\)90046-X](https://doi.org/10.1016/0022-1694(92)90046-X)
- Gao C, Xu Y-P, Zhu Q et al (2018) Stochastic generation of daily rainfall events: A single-site rainfall model with Copula-based joint simulation of rainfall characteristics and classification and simulation of rainfall patterns. *J Hydrol* 564:41–58. <https://doi.org/10.1016/j.jhydrol.2018.06.073>
- Ghamariadyan M, Imteaz MA (2021a) Prediction of Seasonal Rainfall with One-year Lead Time Using Climate Indices: A Wavelet Neural Network Scheme. *Water Resour Manag* 35:5347–5365. <https://doi.org/10.1007/s11269-021-03007-x>
- Ghamariadyan M, Imteaz MA (2021b) Monthly rainfall forecasting using temperature and climate indices through a hybrid method in Queensland, Australia. *J Hydrometeorol* 1259–1273. <https://doi.org/10.1175/JHM-D-20-0169.1>
- Ghamariadyan M, Imteaz MA (2021c) A wavelet artificial neural network method for medium-term rainfall prediction in Queensland (Australia) and the comparisons with conventional methods. *Int J Climatol* 41. <https://doi.org/10.1002/joc.6775>
- Grossmann A, Morlet J (1984) Decomposition of Hardy functions into square integrable wavelets of constant shape. *SIAM J Math Anal* 15:723–736. <https://doi.org/10.1137/0515056>
- Jiang L, Wu J (2013) Hybrid PSO and GA for Neural Network Evolutionary in Monthly Rainfall Forecasting. In: Selamat A, Nguyen NT, Haron H (eds) *Intelligent Information and Database Systems*. ACIIDS 2013. Lecture Notes in Computer Science. Springer, Berlin, Heidelberg, 79–88
- Kalteh AM (2017) Enhanced Monthly Precipitation Forecasting Using Artificial Neural Network and Singular Spectrum Analysis Conjunction Models. *Ina Lett* 2:73–81. <https://doi.org/10.1007/s41403-017-0025-9>
- Kang S, Lin H (2007) Wavelet analysis of hydrological and water quality signals in an agricultural watershed. *J Hydrol* 338:1–14. <https://doi.org/10.1016/j.jhydrol.2007.01.047>
- Ke J, Liu X (2008) Empirical analysis of optimal hidden neurons in neural network modeling for stock prediction. In: 2008 IEEE Pacific-Asia Workshop on Computational Intelligence and Industrial Application. *IEEE* 2:828–832

- Khan MT, Shoaib M, Hammad M et al (2021) Application of Machine Learning Techniques in Rainfall-Runoff Modelling of the Soan River Basin. *Pakistan Water* 13:3528. <https://doi.org/10.3390/w13243528>
- Kisi O, Alizamir M (2018) Modelling reference evapotranspiration using a new wavelet conjunction heuristic method: Wavelet extreme learning machine vs wavelet neural networks. *Agric for Meteorol* 263:41–48. <https://doi.org/10.1016/j.agrformet.2018.08.007>
- Kripalani RH, Inamdar S, Sontakke NA (1996) RAINFALL VARIABILITY OVER BANGLADESH AND NEPAL: COMPARISON AND CONNECTIONS WITH FEATURES OVER INDIA. *Int J Climatol* 16:689–703. [https://doi.org/10.1002/\(SICI\)1097-0088\(199606\)16:6%3c689::AID-JOC36%3e3.0.CO;2-K](https://doi.org/10.1002/(SICI)1097-0088(199606)16:6%3c689::AID-JOC36%3e3.0.CO;2-K)
- Krishna B, Satyaji YR, R, PC N, (2011) Time series modeling of river flow using wavelet neural networks. *J Water Resour Prot* 3:50–59. <https://doi.org/10.4236/jwarp.2011.31006>
- Kumar D, Ch S, Mathur S, Panigrahi BK (2013) Hybrid algorithm performance with varying population size for multi-objective optimisation of in-situ bioremediation of groundwater. *Int J Bio-Inspired Comput* 5:164–174. <https://doi.org/10.1504/IJBIC.2013.055086>
- Kumar S, Tiwari MK, Chatterjee C, Mishra A (2015) Reservoir Inflow Forecasting Using Ensemble Models Based on Neural Networks, Wavelet Analysis and Bootstrap Method. *Water Resour Manag* 29:4863–4883. <https://doi.org/10.1007/s11269-015-1095-7>
- Kumar D, Adamowski J, Suresh R, Ozga-Zielinski B (2016) Estimating Evapotranspiration Using an Extreme Learning Machine Model: Case Study in North Bihar. *India J Irrig Drain Eng* 142:4016032. [https://doi.org/10.1061/\(ASCE\)IR.1943-4774.0001044](https://doi.org/10.1061/(ASCE)IR.1943-4774.0001044)
- Kumar M, Kumari A, Kushwaha DP et al (2020) Estimation of Daily Stage-Discharge Relationship by Using Data-Driven Techniques of a Perennial River. *India Sustainability* 12:7877. <https://doi.org/10.3390/su12197877>
- Kumar M, Kumari A, Kumar D et al (2021) The Superiority of Data-Driven Techniques for Estimation of Daily Pan Evaporation. *Atmosphere (basel)* 12:701. <https://doi.org/10.3390/atmos12060701>
- Kumar D, Singh VK, Abed SA et al (2023) Multi-ahead electrical conductivity forecasting of surface water based on machine learning algorithms. *Appl Water Sci* 13:192. <https://doi.org/10.1007/s13201-023-02005-1>
- Kushwaha NL, Bhardwaj A, Verma VK (2016) Hydrologic response of Takarla-Ballowal watershed in Shivalik foot-hills based on morphometric analysis using remote sensing and GIS. *J Indian Water Resour Soc* 36:17–25
- Kushwaha NL, Rajput J, Elbeltagi A et al (2021) Data Intelligence Model and Meta-Heuristic Algorithms-Based Pan Evaporation Modelling in Two Different Agro-Climatic Zones: A Case Study from Northern India. *Atmosphere (basel)* 12:1654. <https://doi.org/10.3390/atmos12121654>
- Li D (2014) Assessing the impact of interannual variability of precipitation and potential evaporation on evapotranspiration. *Adv Water Resour* 70:1–11. <https://doi.org/10.1016/j.advwatres.2014.04.012>
- Li L, Li W, Barros AP (2013) Atmospheric moisture budget and its regulation of the summer precipitation variability over the Southeastern United States. *Clim Dyn* 41:613–631. <https://doi.org/10.1007/s00382-013-1697-9>
- Li J, Wang Z, Wu X, Xu C, Guo S, Chen X (2020) Toward Monitoring Short-Term Droughts Using a Novel Daily Scale, Standardized Antecedent Precipitation Evapotranspiration Index. *J Hydrometeorology* 21(5):891–908. <https://doi.org/10.1175/JHM-D-19-0298.1>
- Li S, Xie Q, Yang J (2022) Daily suspended sediment forecast by an integrated dynamic neural network. *J Hydrol* 604:127258. <https://doi.org/10.1016/j.jhydrol.2021.127258>
- Lin X, Zhu G, Qiu D, Ye L, Liu Y, Chen L, Sun N (2023) Stable precipitation isotope records of cold wave events in Eurasia. *Atmos Res* 296:107070. <https://doi.org/10.1016/j.atmosres.2023.107070>
- Liu QY, Li DQ, Tang XS, Du W (2023) Predictive Models for Seismic Source Parameters Based on Machine Learning and General Orthogonal Regression Approaches. *Bull Seismol Soc Am* 113(6):2363–2376. <https://doi.org/10.1785/0120230069>
- Lu S, Zhu G, Meng G, Lin X, Liu Y, Qiu D, Jiao Y (2024) Influence of atmospheric circulation on the stable isotope of precipitation in the monsoon margin region. *Atmos. Res.* 298:107131. <https://doi.org/10.1016/j.atmosres.2023.107131>
- Makwana JJ, Tiwari MK (2014) Intermittent Streamflow Forecasting and Extreme Event Modelling using Wavelet based Artificial Neural Networks. *Water Resour Manag* 28:4857–4873. <https://doi.org/10.1007/s11269-014-0781-1>
- Makwana JJ, Tiwari MK (2017) Hydrological stream flow modeling using soil and water assessment tool (SWAT) and neural networks (NNs) for the Limkheda watershed, Gujarat, India. *Model Earth Syst Environ* 3:635–645. <https://doi.org/10.1007/s40808-017-0323-y>
- Markuna S, Kumar P, Ali R et al (2023) Application of Innovative Machine Learning Techniques for Long-Term Rainfall Prediction. *Pure Appl Geophys* 180:335–363. <https://doi.org/10.1007/s00024-022-03189-4>
- McCulloch WS, Pitts W (1943) A logical calculus of the ideas immanent in nervous activity. *Bull Math Biophys* 5:115–133. <https://doi.org/10.1007/BF02478259>
- Mirzania E, Vishwakarma DK, Bui Q-AT et al (2023) A novel hybrid AIG-SVR model for estimating daily reference evapotranspiration. *Arab J Geosci* 16:301. <https://doi.org/10.1007/s12517-023-11387-0>
- Mishra AK, Desai VR (2006) Drought forecasting using feed-forward recursive neural network. *Ecol Modell* 198:127–138. <https://doi.org/10.1016/j.ecolmodel.2006.04.017>
- Nakken M (1999) Wavelet analysis of rainfall–runoff variability isolating climatic from anthropogenic patterns. *Environ Model Softw* 14:283–295. [https://doi.org/10.1016/S1364-8152\(98\)00080-2](https://doi.org/10.1016/S1364-8152(98)00080-2)
- Nourani V (2014) A Review on Applications of Artificial Intelligence-Based Models to Estimate Suspended Sediment Load. *Int J Soft Comput Eng* 3:121–127
- Nourani V, Alami MT, Aminfar MH (2009) A combined neural-wavelet model for prediction of Ligvanchai watershed precipitation. *Eng Appl Artif Intell* 22:466–472. <https://doi.org/10.1016/j.engappai.2008.09.003>
- Oettli P, Camberlin P (2005) Influence of topography on monthly rainfall distribution over East Africa. *Clim Res* 28:199–212. <https://doi.org/10.3354/cr028199>
- Pande CB, Kushwaha NL, Orimoloye I, Kumar R, Abdo HG, Tolche AD, Elbeltagi A (2023) Comparative assessment of improved SVM method under different Kernel functions for predicting Multi scale drought index. *Water Resour Manage.* <https://doi.org/10.1007/s11269-023-03440-0>
- Partal T, Kişi Ö (2007) Wavelet and neuro-fuzzy conjunction model for precipitation forecasting. *J Hydrol* 342:199–212. <https://doi.org/10.1016/j.jhydrol.2007.05.026>
- Pimentel-Gomes F (2023) *Curso de estatística experimental*. Digitaliza Conteúdo, Portuguese Brazilian Edition, Publisher, FEALQ
- Rachmatullah MIC, Santoso J, Surendro K (2021) Determining the number of hidden layer and hidden neuron of neural network for wind speed prediction. *PeerJ Comput Sci* 7:e724. <https://doi.org/10.7717/peerj-cs.724>
- Rautela KS, Kumar D, Gandhi BGR et al (2022) Application of ANNs for the modeling of streamflow, sediment transport, and erosion rate of a high-altitude river system in Western Himalaya, Uttarakhand. *Revista Brasileira de Recursos Hídricos Brazilian Journal*

- of Water Resources 1–15. <https://doi.org/10.1590/2318-0331.272220220045>
- Ray M, Singh KN, Ramasubramanian V et al (2020) Integration of Wavelet Transform with ANN and WNN for Time Series Forecasting: an Application to Indian Monsoon Rainfall. *Natl Acad Sci Lett* 43:509–513. <https://doi.org/10.1007/s40009-020-00887-2>
- Ridwan WM, Sapitang M, Aziz A et al (2021) Rainfall forecasting model using machine learning methods: Case study Terengganu, Malaysia. *Ain Shams Eng J* 12:1651–1663. <https://doi.org/10.1016/j.asej.2020.09.011>
- Roy B, Singh MP, Kaloop MR et al (2021) Data-Driven Approach for Rainfall-Runoff Modelling Using Equilibrium Optimizer Coupled Extreme Learning Machine and Deep Neural Network. *Appl Sci* 11:6238. <https://doi.org/10.3390/app11136238>
- Sahay RR, Srivastava A (2014) Predicting Monsoon Floods in Rivers Embedding Wavelet Transform, Genetic Algorithm and Neural Network. *Water Resour Manag* 28:301–317. <https://doi.org/10.1007/s11269-013-0446-5>
- Samantaray S, Sahoo A, Satapathy DP (2022) Prediction of groundwater-level using novel SVM-ALO, SVM-FOA, and SVM-FFA algorithms at Purba-Medinipur. *India Arab J Geosci* 15:723. <https://doi.org/10.1007/s12517-022-09900-y>
- Sammen SS, Ehteram M, Abba SI et al (2021) A new soft computing model for daily streamflow forecasting. *Stoch Environ Res Risk Assess* 35:2479–2491. <https://doi.org/10.1007/s00477-021-02012-1>
- Santos CAG, Freire PKMM (2012) Analysis of precipitation time series of urban centers of northeastern Brazil using wavelet. *Int J Environ Ecol Geol Min Eng* 6(7):64–69
- Saroughi M, Mirzania E, Vishwakarma DK, et al (2023) A Novel Hybrid Algorithms for Groundwater Level Prediction. *Iran J Sci Technol Trans Civ Eng*. <https://doi.org/10.1007/s40996-023-01068-z>
- Seo Y, Kim S, Kisi O, Singh VP (2015) Daily water level forecasting using wavelet decomposition and artificial intelligence techniques. *J Hydrol* 520:224–243. <https://doi.org/10.1016/j.jhydrol.2014.11.050>
- Sheela KG, Deepa SN (2013) Review on Methods to Fix Number of Hidden Neurons in Neural Networks. *Math Probl Eng* 2013:1–11. <https://doi.org/10.1155/2013/425740>
- Shukla R, Kumar P, Vishwakarma DK, et al (2021) Modeling of stage-discharge using back propagation ANN-, ANFIS-, and WANN-based computing techniques. *Theor Appl Climatol* <https://doi.org/10.1007/s00704-021-03863-y>
- Sihag P (2018) Prediction of unsaturated hydraulic conductivity using fuzzy logic and artificial neural network. *Model Earth Syst Environ* 4:189–198. <https://doi.org/10.1007/s40808-018-0434-0>
- Singh G, Joshi RD, Chopra SK, Singh AB (1974) Late quaternary history of vegetation and climate of the Rajasthan desert, India. *Philos Trans R Soc London b, Biol Sci* 267:467–501. <https://doi.org/10.1098/rstb.1974.0006>
- Singh VK, Panda KC, Sagar A et al (2022) Novel Genetic Algorithm (GA) based hybrid machine learning-pedotransfer Function (ML-PTF) for prediction of spatial pattern of saturated hydraulic conductivity. *Eng Appl Comput Fluid Mech* 16:1082–1099. <https://doi.org/10.1080/19942060.2022.2071994>
- Singh VK, Kumar D, Kashyap PS, Singh PK (2019) Predicting unsaturated hydraulic conductivity of soil based on machine learning algorithms. In: Conference: Proceedings of International Conference Opportunities and Challenges in Engineering, Management and Science (OCEMS- Feb, 2019) At: Bareilly, India
- Smith LC, Turcotte DL, Isacks BL (1998) Stream flow characterization and feature detection using a discrete wavelet transform. *Hydrol Process* 12:233–249. [https://doi.org/10.1002/\(SICI\)1099-1085\(199802\)12:2%3c233::AID-HYP573%3e3.0.CO;2-3](https://doi.org/10.1002/(SICI)1099-1085(199802)12:2%3c233::AID-HYP573%3e3.0.CO;2-3)
- Tan ML, Gassman PW, Yang X, Haywood J (2020) A review of SWAT applications, performance and future needs for simulation of hydro-climatic extremes. *Adv Water Resour* 143:103662. <https://doi.org/10.1016/j.advwatres.2020.103662>
- Tarhule A (2005) Damaging Rainfall and Flooding: The Other Sahel Hazards. *Clim Change* 72:355–377. <https://doi.org/10.1007/s10584-005-6792-4>
- Thomas DSG, Twyman C, Osbahr H, Hewitson B (2007) Adaptation to climate change and variability: farmer responses to intra-seasonal precipitation trends in South Africa. *Clim Change* 83:301–322. <https://doi.org/10.1007/s10584-006-9205-4>
- Tiwari DK, Rautela KS, Tiwari HL, Goyal MK (2023) Artificial Neural Network Models for Rainfall-Runoff Modeling in India: Studies From the Kolar and Kuttiyadi River Watersheds. In: Gupta AK, Goyal MK, Singh SP (eds) *Ecosystem Restoration: Towards Sustainability and Resilient Development*. Disaster Resilience and Green Growth. Springer, Singapore, 201–217
- Trenberth K (2011) Changes in precipitation with climate change. *Clim Res* 47:123–138. <https://doi.org/10.3354/cr00953>
- Tzeng F-Y, Ma K-L (2005) Opening the Black Box - Data Driven Visualization of Neural Networks. In: VIS 05. *IEEE Visualization, 2005*. IEEE 383–390. <https://doi.org/10.1109/VISUAL.2005.1532820>
- Vishwakarma DK, Kumar R, Abed SA et al (2023a) Modeling of soil moisture movement and wetting behavior under point-source trickle irrigation. *Sci Rep* 13:14981. <https://doi.org/10.1038/s41598-023-41435-4>
- Vishwakarma DK, Kuriqi A, Abed SA et al (2023b) Forecasting of stage-discharge in a non-perennial river using machine learning with gamma test. *Heliyon* 9:e16290. <https://doi.org/10.1016/j.heliyon.2023.e16290>
- Vishwakarma DK, Kumar R, Pandey K, et al (2018) Modeling of Rainfall and Ground Water Fluctuation of Gonda District Uttar Pradesh, India. *Int J Curr Microbiol Appl Sci* 7:2613–2618. <https://doi.org/10.20546/ijcmas.2018.705.302>
- White CJ, Tanton TW, Rycroft DW (2014) The Impact of Climate Change on the Water Resources of the Amu Darya Basin in Central Asia. *Water Resour Manag* 28:5267–5281. <https://doi.org/10.1007/s11269-014-0716-x>
- Wu CL, Chau KW, Fan C (2010) Prediction of rainfall time series using modular artificial neural networks coupled with data-preprocessing techniques. *J Hydrol* 389:146–167. <https://doi.org/10.1016/j.jhydrol.2010.05.040>
- Wu X, Guo S, Qian S, Wang Z, Lai C, Li J, ... Liu P, (2022) Long-range precipitation forecast based on multipole and preceding fluctuations of sea surface temperature. *Int J Climatol* 42(15):8024–8039. <https://doi.org/10.1002/joc.7690>
- Zhang BL, Dong ZY (2001) An adaptive neural-wavelet model for short term load forecasting. *Electr Power Syst Res* 59:121–129. [https://doi.org/10.1016/S0378-7796\(01\)00138-9](https://doi.org/10.1016/S0378-7796(01)00138-9)
- Zhang J, Morris AJ (1998) A Sequential Learning Approach for Single Hidden Layer Neural Networks. *Neural Netw* 11:65–80. [https://doi.org/10.1016/S0893-6080\(97\)00111-1](https://doi.org/10.1016/S0893-6080(97)00111-1)
- Zhang W, Peng G, Li C et al (2017) A New Deep Learning Model for Fault Diagnosis with Good Anti-Noise and Domain Adaptation Ability on Raw Vibration Signals. *Sensors* 17:425. <https://doi.org/10.3390/s17020425>
- Zhang S, Bai X, Zhao C, Tan Q, Luo G, Wang J, Xi H (2021) Global CO₂ Consumption by Silicate Rock Chemical Weathering: Its Past and Future. *Earth's Future* 9(5):e1938E-e2020E. <https://doi.org/10.1029/2020EF001938>
- Zhang P, Liu L, Yang L, Zhao J, Li Y, Qi Y, Cao L (2023) Exploring the response of ecosystem service value to land use changes under multiple scenarios coupling a mixed-cell cellular automata model and system dynamics model in Xi'an China. *Ecol Indic* 147:110009. <https://doi.org/10.1016/j.ecolind.2023.110009>

- Zhao L, Liu M, Song Z et al (2022) Regional-scale modeling of rainfall-induced landslides under random rainfall patterns. *Environ Model Softw* 155:105454. <https://doi.org/10.1016/j.envsoft.2022.105454>
- Zhou G, Lin G, Liu Z, Zhou X, Li W, Li X, Deng R (2023) An optical system for suppression of laser echo energy from the water surface on single-band bathymetric LiDAR. *Optics and Lasers in Engineering* 163:107468. <https://doi.org/10.1016/j.optlaseng.2022.107468>
- Zhou G, Wu G, Zhou X, Xu C, Zhao D, Lin J, Zhang L (2023) Adaptive model for the water depth bias correction of bathymetric LiDAR point cloud data. *Int J Appl Earth Obs Geoinf* 118:103253. <https://doi.org/10.1016/j.jag.2023.1032>
- Ziervogel G, Johnston P, Matthew M, Mukheibir P (2010) Using climate information for supporting climate change adaptation in water resource management in South Africa. *Clim Change* 103:537–554. <https://doi.org/10.1007/s10584-009-9771-3>

Publisher's Note Springer Nature remains neutral with regard to jurisdictional claims in published maps and institutional affiliations.

Springer Nature or its licensor (e.g. a society or other partner) holds exclusive rights to this article under a publishing agreement with the author(s) or other rightsholder(s); author self-archiving of the accepted manuscript version of this article is solely governed by the terms of such publishing agreement and applicable law.